Friction
https://doi.org/10.1007/s40544-024-0865-8
ISSN 2223-7690
CN 10-1237/TH
RESEARCH ARTICLE

Pressurized environments directly influence friction and wear of dry steel contacts—Investigations in a novel high fluid pressure tribometer

Paul REICHLE[1,2,*], **Jakob BARZ**[1,2], **Georg UMLAUF**[2], **Günter E.M. TOVAR**[1,2,*]

[1] *Institute of Interfacial Process Engineering and Plasma Technology (IGVP), University of Stuttgart, Stuttgart 70569, Germany*

[2] *Fraunhofer Institute for Interfacial Engineering and Biotechnology (IGB), Stuttgart 70569, Germany*

Received: 09 June 2023 / Revised: 23 September 2023 / Accepted: 18 December 2023

Abstract: To reduce the usage of classical lubricants in deep drawing, a new tribological system based on volatile lubricants was developed. Therefore, a volatile medium is injected under high pressure into the interstice between drawing tool and sheet metal. Depending on temperature and pressure, the temporary lubricant may exist in its gaseous or liquid phase. In this study, a novel high fluid pressure tribometer was designed to investigate the friction and wear of dry steel contacts under comparable conditions like in dry deep drawing. Therefore, a new ball-on-disc tribometer was designed and integrated into a high-pressure vessel. To specifically investigate the effects of different environments (technical air, liquid and gaseous carbon dioxide, nitrogen, argon) at atmospheric and high pressure (0.1 MPa, 6 MPa) on tribology, the specimens and all components were operating unlubricated. During the experiments, the friction was measured continuously. Results show that the highest friction occurs in air and the lowest in carbon dioxide environment. Subsequent to the experiments, the wear of the specimens was assessed along with changes in surface chemistry related to tribochemical reactions. Therefore, the tribology of the dry sliding contacts is correlated to changes of the surface chemistry. Also differences as well as similarities regarding the different fluid environments are shown. As the results show, the differences between the media used are most pronounced at elevated pressure. Concluding, this work gives clear indications on the suitability of volatile lubricants in dry friction or rather gas lubrication, especially for dry deep drawing.

Keywords: dry friction and dry wear; gas lubrication; carbon dioxide; tribo-layer; dry metal forming

1 Introduction

Reducing friction and wear is a widespread aim of nearly every scientific field where opposite motion of bodies occurs. Commonly, a wide range of oils, emulsions, waxes or solid lubricants is used to achieve this aim. In principle, lubricants wet or cover the surfaces of the bodies, which are in relative motion against each other in order to control, sometimes even prevent, direct contact of the solids and thus allow defined sliding conditions. For a proper and matched lubrication, the used substances usually contain various additives. As many of these additives and the lubricants itself are harmful to humans and the environment, science is searching for new ecofriendly lubricants [1–4]. Moreover, technologies are developed to reduce the amount of used lubricant, since the previous lubricant application and cleaning steps subsequent to, for instance forming processes are time and cost-intensive [5–7]. A further going approach, without any need of conventional lubricants is the usage of volatile lubricants. Regarding deep drawing processes, a new technique was developed where volatile substances are introduced under high pressure

* Corresponding authors: Paul REICHLE, E-mail: paul.reichle@igvp.uni-stuttgart.de; Günter E.M. TOVAR, E-mail: guenter.tovar@igvp.uni-stuttgart.de

into the forming zone via laser drilled micro injectors in the drawing tool [8–10]. Comparable to a hydrostatic gas bearing, the injected fluid separates the counter bodies and acts as a temporary lubricant. The investigations showed a high dependency between the flow behavior of the media and the tribology in the drawing process [8, 11]. However, since Bowden and Hughes [12], Iwabuchi et al. [13] and Mishina [14, 15] started the research on dry sliding metal contacts in different atmospheres, a connection between gas environment and tribological behavior is obvious. Several studies followed, investigating the influence of different gaseous or volatile media on the tribology of sliding contacts [16–18]. In cryogenic machining a variety of different volatile lubricants like liquid carbon dioxide, -nitrogen or -helium are used [19, 20]. Having said this, here the focus is on reducing friction and wear by decreasing temperature. At room temperature, Velkavrh et al. [21] examined the influence of different technical gas atmospheres on the tribology of dry steel contacts and the formation of adsorbed surface layers from the gas phase. As shown in diverse studies, the adsorption is dependent on atmospheric conditions like temperature and fluid pressure [22, 23]. Thus, it is assumed that the gas atmosphere pressure has an essential effect on the tribology of dry sliding contacts. However, only few investigations were made so far to identify the influence of the fluid pressure above 0.1 MPa on the tribology [24–28]. These studies mainly focus on the behavior of carbon dioxide (CO_2) as it changes its state at room temperature at approx. 6 MPa pressure from gaseous to liquid (see Fig. 1) and can be used as a refrigerant. The present study investigates the influence of different environments: technical dry air, gaseous CO_2 (GCO_2), liquid CO_2 (LCO_2), nitrogen (N_2) and argon (Ar) at room temperature and two fluid pressure levels (p_F = 0.1 MPa and p_F = 6 MPa) on the tribological behavior of dry sliding steel–steel contacts. Therefore, a novel high-pressure tribometer was designed (see Chapter 2.1). The friction between the tool steel specimens was measured during the investigations and wear was classified afterwards (see Chapters 3.1 and 3.2). To examine chemical changes of the specimen surfaces as a result of wear as well as reactions and adsorption processes of the lubrication fluid, scanning electron microscopy (SEM) along with energy dispersive X-ray spectroscopy (EDX) and X-ray photoelectron spectroscopy (XPS) measurements were performed (see Chapter 3.3).

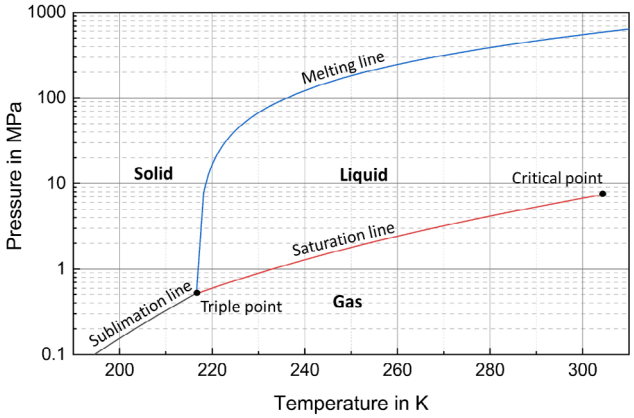

Fig. 1 Phase diagram of carbon dioxide; shown as it changes its state at room temperature at approx. 6 MPa from gaseous to lipid. Reproduced with permission from Ref. [11], © The Author(s) 2021, and adapted from Ref. [29], © ChemicaLogic Corporation 1999.

2 Methods and procedures

The majority of the mentioned research groups, who investigated the influence of the atmosphere on tribology of dry metal contacts, used customary tribometer setups placed in a sealed box to control the environment. However, for high fluid pressure applications, no commercial tribometer is available and pressurized containers must be designed according to special standards for safety reasons. Thus, a new tribometer was designed (inspired by Refs. [27, 30, 31]), matching a customary high-pressure vessel.

2.1 Design of the high-pressure tribometer

As for exchanging the samples, the used pressure vessel has to be opened after each experiment, it was decided to use a volume as small as possible to prevent unnecessary fluid loss. For this purpose, the midiclave Type 4 (Büchi AG; Switzerland) high-pressure vessel with 1 L capacity and a pressure range up to 20 MPa was used. In Fig. 2, a model of the designed tribometer and pressure vessel ① is shown. As the casing is performed double-walled with a built-in temperature control coil ⑧, almost constant room temperature (296 K) for all examinations can be achieved. For the needed motion inside the

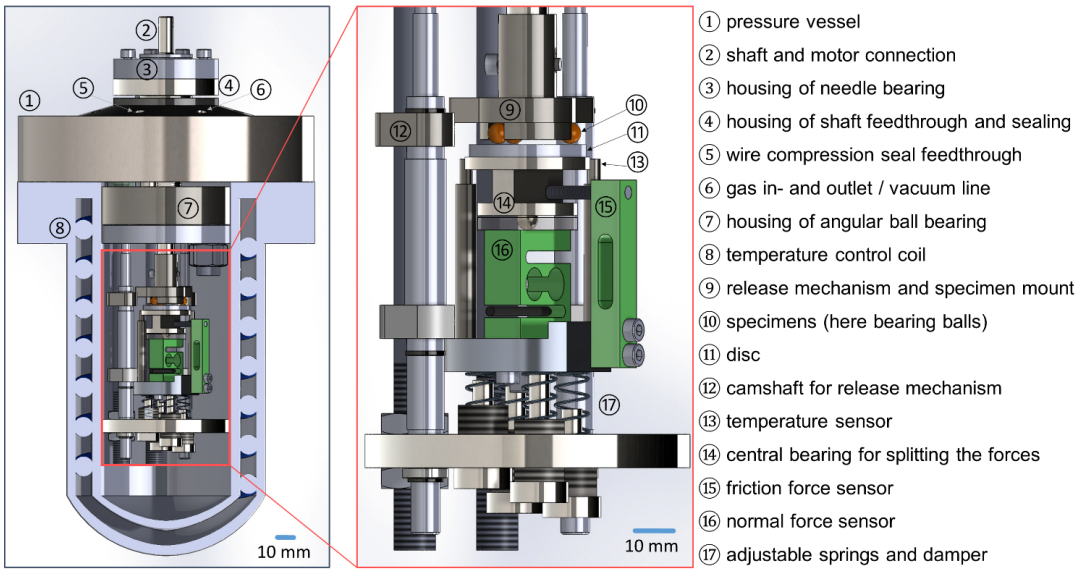

Fig. 2 Computer-aided 3D-model of the pressure vessel (partial cross section) and the labeling of the tribometer components (modeled with SolidWorks).

vessel, a shaft ② is integrated. On the outer side of the shaft, a motor, and on the inner side, an interface for a specimen mount can be connected. On the shaft, a position sensor is installed to measure the sliding distance. For the utilization with high fluid pressures, a special feedthrough ④ for the shaft was designed. To ensure a proper sealing of the feedthrough, a needle bearing ③ centers the shaft. As the pressure inside the vessel pushes the shaft outward, an angular ball bearing is mounted ⑦ to prevent motion in this direction. To ensure the dry sliding conditions and to prevent any contamination of the vessel, the bearings are working unlubricated. The data cables for the sensors and the power supply are also sealed by a wire compression feedthrough ⑤. For the gas inlet and outlet as well as the pressure measurement during the investigations, the same connection can be used ⑥. To fix the specimens, a universal mount was designed ⑨ for either balls or pins. In this study, consistently balls ⑩ were used and fixed by a strong clamp to prevent them from turning. As counter body, a disc ⑪ can be installed. The disc is fixed on a measuring assemblage ⑭, splitting the forces for a friction force sensor ⑮ and the normal force sensor ⑯. To measure the sample temperature, a temperature sensor ⑬ is placed nearby. For the adjustment and variation of the applied normal force, four springs and damper are installed ⑰. In the experiments of this work, a normal force (F_N) of 3 N was constantly applied (see Fig. 3). As previous investigations had shown, force sensors exhibit a set off when exposed to high gas pressure. Thus, a mechanism ⑫ was designed to enable a reset of the sensors after setting F_N and applying the fluid pressure. Therefore, it is now possible to measure the absolute and relative normal force independently of the environmental pressure. In addition, the mechanism also allows a separation of the samples before starting the motion to ensure a homogeneous wetting e.g. gas adsorption on the surfaces and to avoid static friction at the beginning of each experiment. In order to prevent an asymmetrical distribution of forces, three balls are arranged at an angle of 120° to one another, effecting contact to the disc at those three locations (see Fig. 3). As the disc is slightly tiltable and the three balls define the contact plane, a permanent contact between balls and disc is realized. The movability of the disc in vertical direction in combination with F_N ensures a constant contact even when the specimens wear out. The normal force at every single ball F_b and the rotation of the balls trigger the friction force F_r trying to turn the disc as well. This motion is inhibited and the needed force F_f can be measured by the friction force sensor for all three sliding contacts in total.

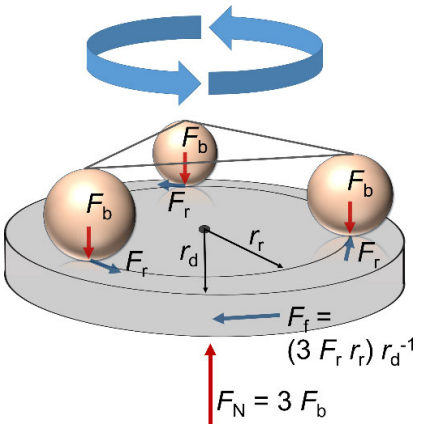

Fig. 3 Schematic illustration of the active forces at the specimens during friction measurement (tangential friction force F_f and central normal force F_N).

2.2 Basic conditions to investigate dry friction

In Table 1, an overview of the parameters used in the investigations and of the tribometer is shown. For the balls the material *100Cr6* (*1.3505*) was used as it is a standard bearing material and was used in several other investigations as well (exemplary Refs. [32–34]). The balls were produced according to the German standard DIN 5401:2002–08 [35] with a diameter of $d_a = 5 \pm 0.00975$ mm, a surface roughness $R_a \leq 0.02$ µm and a hardness of approx. 820 HV10. The disc was made from tool steel *X155CrVMo12–1* (*1.2379*) as it is a broadly used material for forming-, cutting- or roller tools and this work arose from the studies on dry metal forming with volatile lubricants (see Chapter 1 and Ref. [36]). The surface was fine grinded, comparable to used drawing tools with a surface roughness of $R_a \leq 0.3$ µm ($R_z \leq 5$ µm) and a surface hardness of approx. 380 HV10 (hard on soft sliding contact).

The specimens were cleaned and dried prior to the experiments to remove most of lubricant residues and contaminations. To minimize the impact of atmospheric residues on the investigations, the whole vessel was evacuated to pressures below 10^3 Pa and flooded afterwards up to 2×10^5 Pa with pure gas from the gas cylinder for four times prior to each experiment. In addition, the vacuum was to support physical desorption processes of e.g. water and volatile organic compounds (VOCs) on the surfaces of the vessel and the tribometer. This purification can also be seen in the pressure and temperature curve illustrated in part (a) of Fig. 4 exemplarily shown for a gaseous lubricant. The behavior of LCO_2 differs slightly from the shown gaseous media, since the fluid evaporates as long as the chamber pressure is below the saturation line of CO_2 (see Fig. 1). Thus, there is a temperature drop down to approx. 285 K instead of the shown increase (in part (b) of Fig. 4). With LCO_2 the vessel is usually filled until the samples are completely wetted and underneath the surface of the fluid. Independently of the state of the medium, the temperature control ensures temperatures around 296 K after a short period, and the temperature stays almost constant during the tribological investigation (see part (c) in Fig. 4). As soon as this condition is reached, the rotation of the specimens is started. Besides some extended experiments, the first 400 revolutions (about 670 seconds or 37.7 m sliding distance) of the samples were investigated for this study. After each run and before opening the vessel, the media has to be drained until atmospheric pressure is reached (part (d) in Fig. 4).

Table 1 Constant parameters of all experiments.

Normal force, F_N in N	3
Installed balls	3
Ball diameter, d_a in mm	5
Friction radius, r_r in mm	15
Frequency in s^{-1}	0.6
Sliding speed in mm·s^{-1}	56.5
Investigated time in s	670, (if not described differently)
Material balls	100Cr6 (AISI 52100)
Material disc	X155CrVMo12-1 (AISI D2)
Temperature	RT (approx. 296 K)

With $F_N = 3$ N, the Herzian pressure at the beginning of each experiment (no wear e.g. flattening of the ball) is around 750 N·mm^{-2}. Hence, there is no plastic deformation of the balls or the disc but the pressure is still high enough to receive measurable wear and to break through the assumed thin surface layer of residues and oxides.

The used fluids had minimum technical purity (>99.7 vol%) and were directly extracted from the gas cylinder via pressure reducer. The LCO_2 was directly extracted from the gas cylinder at room temperature

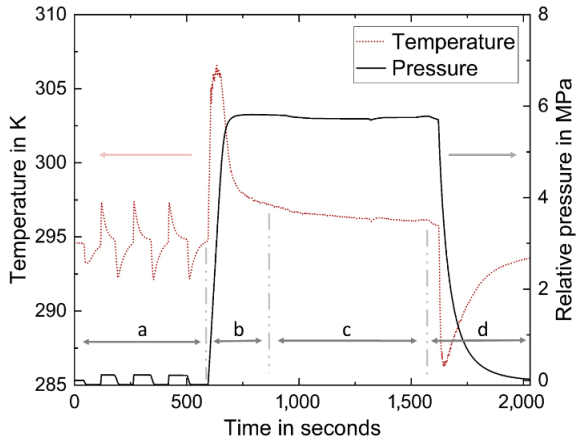

Fig. 4 Exemplary temperature and pressure curve of an examination with nitrogen at p_F = 6 MPa—(a) four evacuating and three flushing processes of the vessel; (b) filling process; (c) approx. constant temperature and pressure for the tribological examination and (d) deflation process.

via riser pipe. Technical air with a composition of 20.5 vol% oxygen and 79.5 vol% N_2 was used (remaining content of water below 2 ppm). The connection between gas cylinder and pressure vessel was evacuated and flushed after every change of the medium for several times.

2.3 Methods to assess wear

Besides the friction measurements, the wear of the samples was assessed. Therefore, the diameter of the flattening of the balls was measured after each investigation using light microscopy. By means of these measurements and the known ball radius, the worn material volume W_v can be calculated. In combination with the measured normal force F_N and the sliding distance s, the wear rate k can be determined according to equation (1): $k = 3\ W_v\ (F_N\ s)^{-1}$.

To assess wear of the discs, the wear tracks were evaluated and the maximum peak to valley 3D surface roughness S_z was measured after ISO 25178 using the 3D confocal microscope μsurf mobile (Nanofocus, Germany). The measuring spot was focused on the wear track with a spot size of 2.56 mm². The measuring accuracy can be estimated on the basis of the measuring uncertainty (calibrated according to German standard VDE/VDI 2655-1.2) and the repeatability to a deviation of ±0.06 μm. Furthermore, scanning electron microscope (SEM) images of selected samples were made.

2.4 Chemical analysis of worn surfaces

To investigate the lubrication effects, chemical analyses of the worn specimens were performed. As the measurement of the disc surface would be very laborious because of space requirements in the measuring device, only the balls were examined. To get a better understanding of the processes during the sliding, energy-dispersive X-ray spectroscopy (EDX) measurements of the worn ball surfaces as well as of the formed wear debris were performed. In addition, X-ray photoelectron spectroscopy (XPS) measurements of the worn ball surfaces were carried out as they give more information about the chemical compounds of the surface. Having said this, XPS yields information of the upper 5 nm to 10 nm whereas EDX reaches a depth in the micrometer range. For all three, the SEM, the EDX, and XPS measurements, an Axis Supra (Kratos - Shimadzu; UK - Japan) was used.

3 Experimental results

3.1 Friction in different media at atmospheric and high pressure conditions

As mentioned, the friction force F_f as well as the applied normal force F_N was measured continuously during the tribometer experiments. In accordance with the Coulomb friction model, the ratio of these two values is the coefficient of friction (CoF, μ), plotted in Fig. 5 for the different environmental conditions. For a higher significance, all examinations were performed at least three times. The faint colored lines show the curves of the experiment with minimum and maximum measured CoF (representing the variance), respectively. The saturated line in the middle represents the arithmetic mean value of all investigations in this category in dependence of the time.

The sliding in air environment showed independently of the fluid pressure the highest measured CoF. At high pressure, a sharp increase could be determined in the first 100 seconds of the examinations. In case of atmospheric pressure, this increase took place as well, in roughly 600 seconds and thus, significantly slower. At the beginning of the experiments, the minimum and maximum values were very close to the mean value, indicating a reproducible friction behavior.

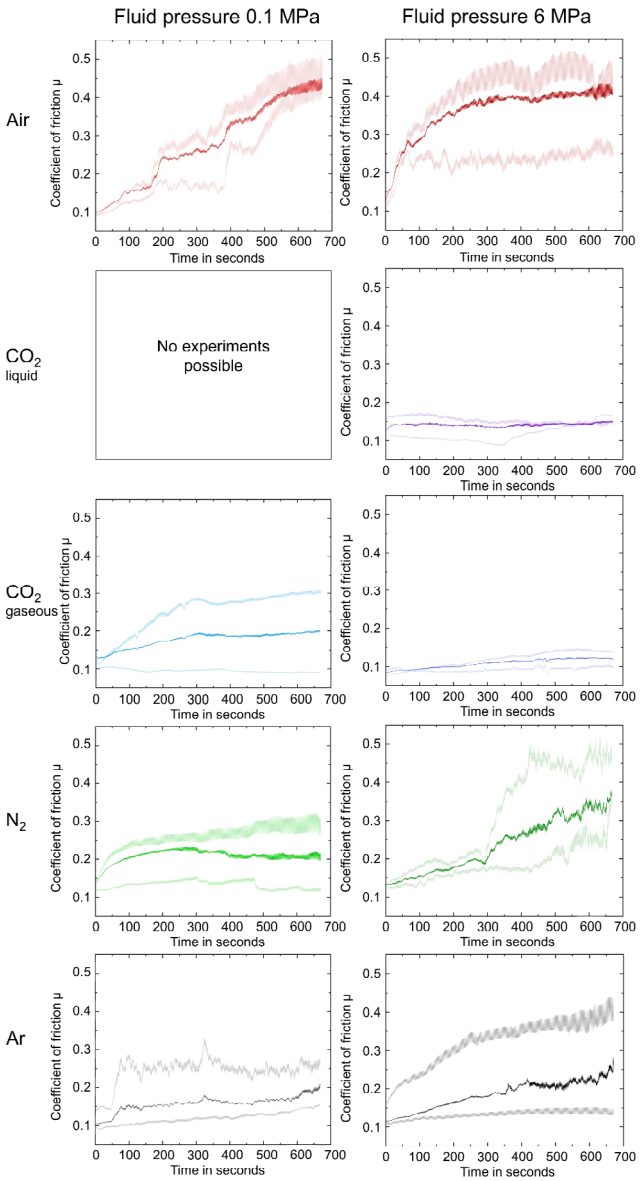

Fig. 5 Coefficients of friction measured in different environments (left row: p_F = 0.1 MPa; right row: p_F = 6 MPa). The faint colored lines indicate the variance, as the curves represent the investigations with minimum and maximum CoF. The saturated line in the middle shows the arithmetic mean value of all investigations at the same time and conditions.

In contrast, after approx. 200 seconds at low fluid pressure and even faster at high pressure, the CoF was getting more and more unstable; marked by an oscillation of the CoF of about ±0.07 and sudden steps.

With LCO_2, no investigation at atmospheric pressure was possible (see Fig. 1). In high fluid pressure, a comparable low CoF was determined. Furthermore, no significant increase within the investigated time could be seen and the CoF stayed almost without any oscillation. A similar behavior could be seen when using GCO_2 at 6 MPa. With a mean CoF below 0.15, the lowest values of all investigations, with only slight increase over time, were measured. By contrast, in a CO_2 environment at atmospheric pressure, the CoF of most of the investigations increased clearly over time. However, the experiment with the lowest friction was comparable to the experiments at 6 MPa (LCO_2 or GCO_2). The examination in 0.1 MPa CO_2 with the highest measured values showed in contrast a friction behavior comparable to those of N_2 or Ar.

At the low N_2 pressure, the friction increased immediately after the start for most investigations. Only one experiment showed no significant increase of the friction over the measuring time. At high N_2 pressure, the CoF increased constantly at the beginning of the examination. After approx. 300 seconds, the CoF increased significantly again, resulting in a more unstable regime as well. Here, the trial with the highest measured friction at 6 MPa fluid pressure reached values comparable to those in air environment. When comparing the friction in N_2 and Ar atmosphere, a similar behavior was determined. For the two gases, the friction at high gas pressure tended to be higher than that at atmospheric pressure.

3.2 Wear of the specimens tested under different atmospheric conditions

To investigate lubrication effects of the different pressurized environments, wear of the specimens was assessed subsequently to the tribometer experiments. During the experiments, the balls were fixed on the specimen mount preventing them to rotate, respectively to roll over the disc. Thus, the balls were flattened at the contact zone. By measuring this flattening diameter, the worn volume of the balls could be calculated (see Chapters 2.3 and 3.2.1). The wear of the discs was assessed by surface roughness, measured via 3D confocal microscope (see Chapter 3.2.2).

3.2.1 Wear of the balls

In Fig. 6, the flattening of a ball is shown exemplarily for each atmosphere. In the case of air condition, the specimens showed heavy wear and a brownish color in the contact area. The direction of motion during

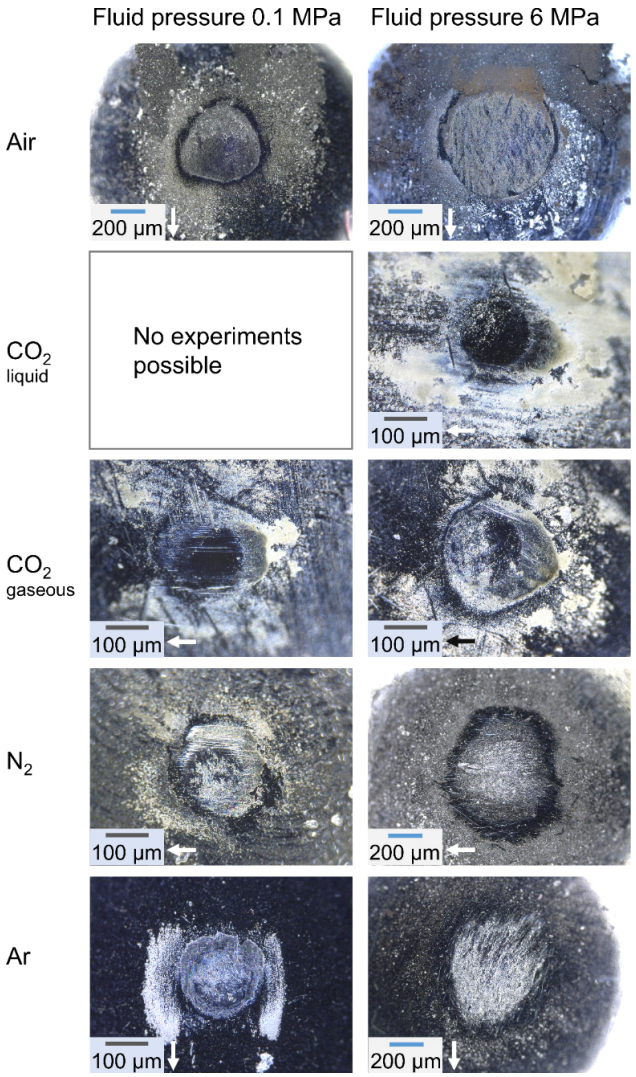

Fig. 6 Wear at the specimen balls, worn in different atmospheres, exemplarily shown for each condition (The arrows indicate the sliding direction. Note the two different magnifications).

the examinations could be seen by means of the small brownish debris formation behind the contact zone. The mentioned observations were even more pronounced when increasing the gas pressure.

With LCO_2, at 6 MPa fluid pressure, small contact zones were observable compared to other experiments, indicating only mild wear. Mainly small debris with a whitish color could be seen. The debris were primarily located behind the contact zone in sliding direction like when using GCO_2. In GCO_2, the size of the contact zone was, compared to air environment, distinctly smaller.

In N_2 atmosphere, at ambient pressure, the debris had more a metallic appearance, were larger in size and located all around the contact zone. The flattening itself was slightly bigger than those worn in CO_2 atmosphere, but significantly smaller than those of air. In high pressure N_2 atmosphere, the number of debris, found on the balls, was lower compared to most other examinations, nevertheless the debris were bigger in size (rather flakes). In addition, instead of a clear flattening of the ball a completely reshaped, rough surface could be seen on a large scale.

Similar observations were made in 6 MPa Ar atmosphere; only the debris formation was slightly higher, with a shiny metallic appearance. The debris were located all around the contact zone. In contrast, in 0.1 MPa Ar environment, the flattening was visible and showed whitish, shiny metallic debris around the contact zone (see Fig. 6).

The wear of single balls, exemplarily shown and annotated in Fig. 6, were collected and measured for all specimens and across all investigations. Therefore, the wear rate k was calculated (see Eq. 1 in Chapter 2.3) as shown in Fig. 7. With $k = 4.09 \times 10^{-5}$ mm³·(N·m)$^{-1}$ in pressurized air atmosphere, the highest wear among all other examinations was measured. It is notable that the wear rate at the high air pressure was more than four times higher than the one at low fluid pressure. The standard deviation of these values is not visible in the graph because of the logarithmic scale of the y-axis and a high reproducibility of the experiments.

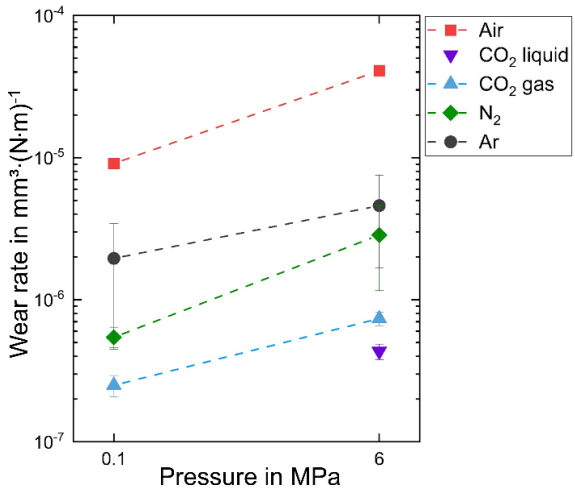

Fig. 7 Illustration of the wear rate of the specimens worn in different media and pressure levels (note the logarithmic scale on y-axis, dashed lines only to guide the eye, and error bars ± sample standard deviation).

In contrast, the variance for the examinations in Ar and N_2 environment were very high. For both gases, an increase of the wear by increasing fluid pressure could be assumed. In addition, a lower wear by using N_2 compared to Ar could be noted; though, the differences were not significant as the reproducibility of those examinations was poor.

Lower wear was measured on the specimens tested in CO_2 atmospheres. With $k = 5 \times 10^{-7}$ mm³·(N·m)$^{-1}$, the lowest wear of all experiments was evaluated in 0.1 MPa GCO_2 environment. At the higher 6 MPa GCO_2 pressure level the wear was likewise increasing. By using LCO_2, a lower wear compared to the gaseous state at the high pressure level and slightly higher than the one at ambient pressure was measured.

3.2.2 *Wear of the disc*

Although the sliding distance of the specimen balls is considerably higher (approx. 210:1) than the one of the counterpart, the wear of the discs was investigated as well. Therefore, Fig. 8 shows a picture of the whole disc, a magnified light microscopy image of a part of

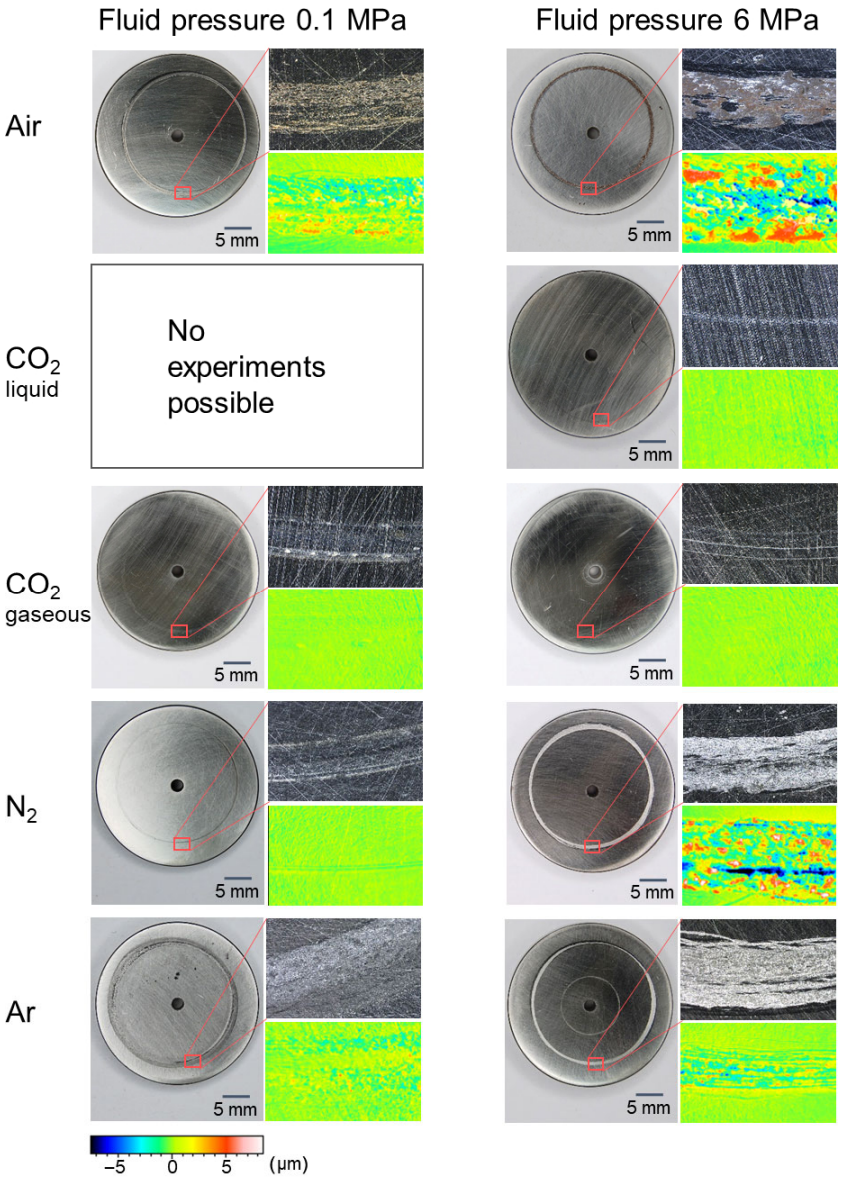

Fig. 8 Compilation of light microscopy images and 3D topographic depictions measured by confocal coherence microscopy of worn discs, tested in different atmospheres. For reasons of comparability, the same magnitude of all topographic pictures was used, therefore at very rough surfaces single roughness peaks or furrows are out of range.

the wear track and a 3D topographic roughness picture of this area, exemplary for each examined condition. Comparable to the wear on the balls (Chapter 3.2.1), the discs tested in air environment showed high wear and a brownish color of the wear tracks as well. Especially after testing in high air pressure, a strong roughening of the surface was determined.

In CO_2 atmosphere only a faint line of wear was visible on the disc surfaces. In addition, the 3D images showed no roughening of the surface.

In case of N_2 atmospheres, different observations were made: In 0.1 MPa atmosphere, mainly low wear was identified; in contrast, at 6 MPa N_2 pressure, wear tracks were clearly visible. The worn surface appeared as glossy bare metal with no discoloration. Deep scratches, material removals and roughness peaks with a height of around 8 µm demonstrated heavy wear and a complete restructuring of the surface.

In Ar environment, effects comparable to those of N_2 were obtained (potentially higher wear at high fluid pressure). However, for N_2 as well as for Ar at low fluid pressure, also examinations with high wear occurred and in turn at the high pressure level experiments with low wear were obtained. Hence, the low reproducibility, as mentioned, regarding the wear of the balls and the CoF can be stated for the assessment of wear of the discs as well.

The previously described wear on the discs (Fig. 8) can also be illustrated in maximum peak to valley area surface roughness S_z as shown in Fig. 9. The measured values mostly confirm the described differences between wear in different pressurized atmospheres. The highest roughness occurred in air followed by N_2 and Ar environment. In these atmospheres, the roughness was significantly increasing at high fluid pressure. In contrast, in CO_2 environment, a lower roughness than the reference was measured after the experiments and no increase with rising fluid pressure could be obtained.

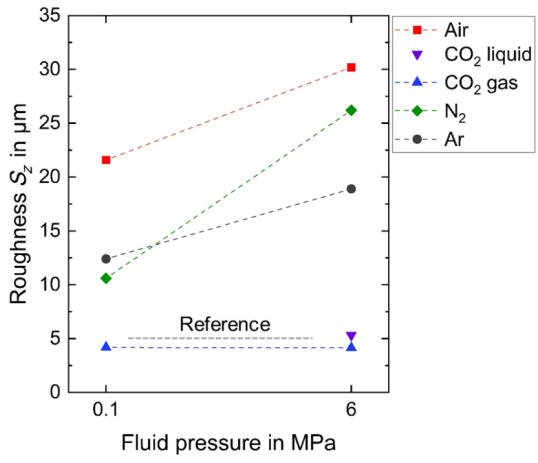

Fig. 9 Maximum peak to valley area surface roughness measured on the sliding tracks on discs worn in different atmospheres. For a better comparability, also the reference level (unused disc surface) is shown (dashed lines only to guide the eye).

3.3 Chemical analyses of worn surfaces

To investigate the effects during sliding, chemical analyses of the worn specimens were performed. In Fig. 10, the results of the elemental composition according to EDX measurements are shown in atomic percentage (at%). In comparison to the reference (cleaned ball before the experiment), the oxygen content of the worn surface and especially of the wear debris increased significantly after the tribotest in air atmosphere. In a similar relation, the carbon and iron content of the surface decreased by wearing in air environment.

The surfaces worn in CO_2 atmosphere showed higher amounts of oxygen, too. In contrast, here the carbon content increased significantly compared to the reference and all other tested specimens.

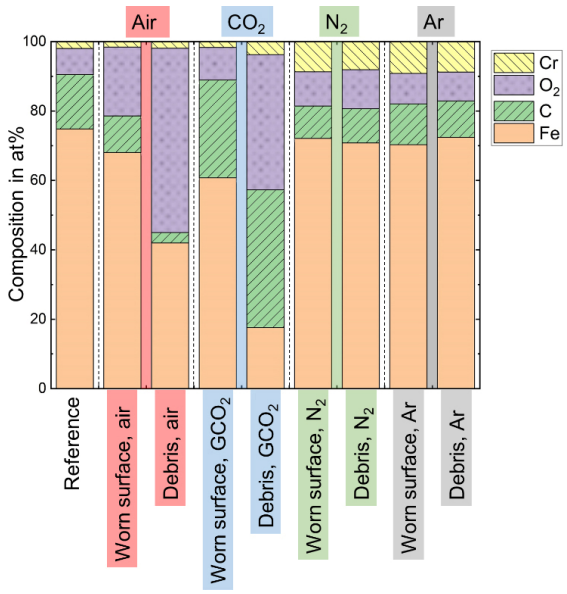

Fig. 10 Results of EDX surface analysis for the elements chromium, oxygen, carbon and iron at different locations of the specimens, before (reference) and after the tests in various environments at p_F = 6 MPa.

The chemical composition of the worn specimen surfaces in N_2 and Ar atmosphere were very much alike. In comparison to the reference, the upper surface layers of these specimens contained more chromium. Furthermore, no distinct differences between the composition of the worn surfaces and the wear debris were detected.

Since the EDX measurements gave fundamental information on the surface elements, but no further classifications regarding compounds could be made, additional XPS measurements were executed. In Fig. 11, the XPS spectra measured at the worn surfaces of the balls (contact zone) are shown for the typical areas of the primarily found elements. The C 1s spectrum of carbon was fitted by four curves with maxima at 282.4 eV, 284.6 eV, 286.8 eV and 289 eV relatable to metallic carbides [37], hydrocarbons [38], other carbon compounds with oxygen [39] and carbonates [40], respectively. The O 1s oxygen spectrum was split into three sub peaks, first at 530 eV allocated to metal oxides mainly Fe_2O_3 and Cr_2O_3 [41]. The second oxygen peak, related to carbonates (primary $FeCO_3$) was located at 531.9 eV and the third at 533.1 eV was assigned to different contaminations like SiO_2, residual alcohols or esters [39, 40, 42]. The iron spectra was fitted by two curves with maxima at 706.3 eV and 709.8 eV, assigned to bare iron as well as iron oxides and carbonates respectively [42]. In Table 2, the quantification of the mentioned elements can be seen. Beside these elements, also small amounts of nitrogen, silicon and steel alloy elements (Cr, Mn, Mo, V) were found. In the mentioned Table 2 only nitrogen and chromium are listed additionally, since they are indicators for material transfers from the disc to the balls and potential surface adsorption layer. As the surfaces consisted of a variety of different compounds as well as atmospheric contaminants and residues from production process, an exact allocation of the spectra and compounds within this investigation was not possible.

In general, a relatively high contamination of hydrocarbons for all samples was measured. The specimens worn in air atmosphere showed in comparison to the other samples the highest amount

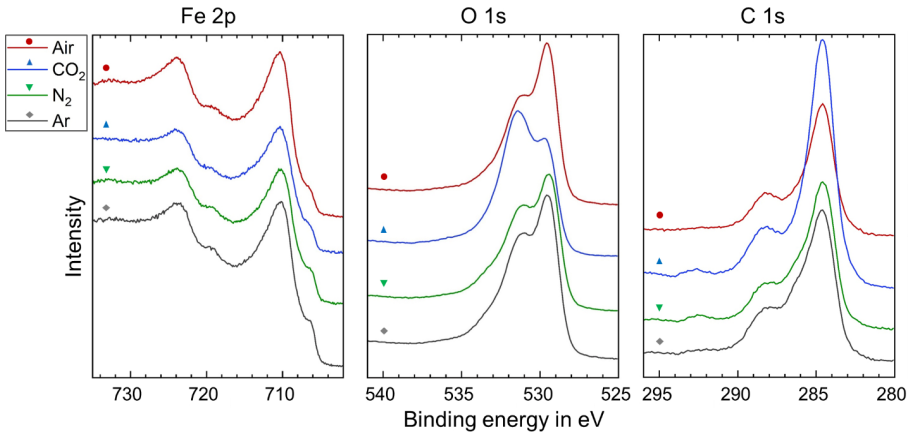

Fig. 11 XPS spectra for selected elements (iron, oxygen, carbon) of specimens contact zones worn in different gaseous atmospheres at p_F = 6 MPa.

Table 2 Quantification of the elements (carbon, oxygen, nitrogen, iron, chromium) of ball surfaces worn in different environments at p_F = 6 MPa, measured via XPS (data in atom percentage).

Element / Lubricant	C metallic carbides	C hydro-carbons	C oxygen comp.	C carbo-nates	O metallic oxides	O carbo-nates	O carbon comp.	N	Fe bare	Fe oxide	Cr oxide
Air	0.6	25.2	11.5	6	31.1	7.9	3.4	1.7	0.5	11.5	0.6
GCO_2	0.4	39.7	7.5	8.4	20.7	9.8	3.6	1.6	0.3	7.1	0.8
N_2	0.4	26	14.1	7.2	26.5	8.1	4.1	3	0.7	8.7	1.2
Ar	0.5	24.1	16.1	5.6	27.4	8	3.8	3	0.8	9.3	1.3

of metallic oxides and in connection the highest value of iron oxides. Except of the chromium content, the other quantities were very similar to the ones measured on the samples worn in Ar and N_2 environment. With over 1.2 atom percentage, the highest amounts of chromium were measured after the wear tests in Ar and N_2 environments. Beside the mentioned differences, the balls worn in CO_2 atmosphere showed—in comparison to the other specimens—the highest values of hydrocarbons and carbonates, and in turn the lowest values of metallic oxygen or rather iron oxides.

4 Discussion of lubrication effects in different environments

As described in the previous sections, friction and wear effects of dry sliding steel contacts at high fluid pressures could be investigated using a novel tribometer. It was possible to study the tribology in technical air, L- and GCO_2, N_2 and Ar environments at 0.1 MPa and 6 MPa fluid pressure. The friction measurements as described in detail in Chapter 3.1 show significant differences regarding the environmental media. The lowest CoF was measured in GCO_2 at 6 MPa atmospheric pressure (median μ = 0.11). In contrast, the highest CoF was measured in air at 6 MPa atmospheric pressure (median μ = 0.38). In Fig. 12, the CoF of all measurements over the whole time of the experiments are summarized. Since the CoF at the beginning of each experiment is approx. equal around 0.15, the lower level of the 1.5 interquartile range (Q1-1.5 IQR; lower level of the mean 99.3% of the data, see Ref. [43]) for most of the trials starts around this value. Only the before mentioned lowest and highest measured CoF in GCO_2 and air atmosphere differ significantly from this value, indicating tribological effects directly at the beginning of the experiments. In case of air, the rise of the CoF is fast, so the values around 0.15 are not included in the 99.3% of here shown data (see variance in Fig. 5). In case of GCO_2, the measured CoF stayed almost constant below 0.15, indicating a permanent lubrication. The marked effects are discussed separately for each media and in more detail subsequently.

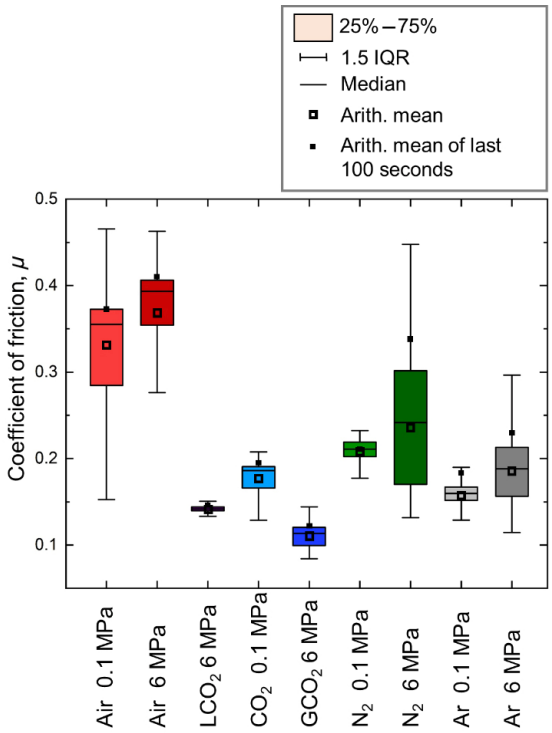

Fig. 12 Summary of the CoF for the investigated environments (inertness rising to the right) analyzed over the time of the experiments and illustrated for different values of statistics (interquartile range IQR).

4.1 Tribological effects in air environment

In air environment, besides the highest CoF also the highest wear rate (see Chapters 3.1 and 3.2.1) was measured. In combination with the results of the experiments in N_2, the essential influence of oxygen on the tribological behavior is obvious. Since oxygen has the predilection to adsorb on metal surfaces [15], the arising surface layers trigger the ejection of wear debris from the contact zone, leading to increased wear. Furthermore, oxidation–reductions occur at the mechanically loaded areas, which is thus a perfect example for tribocorrosion effects. In first prospective, metal oxides usually trigger lower CoF values compared to bare metal surfaces [12, 16, 44]. However, in the second prospective, oxygen causes a faster removal of the surface top layer (debris formation), and thus prematurely results in increasing CoF values [21]. Within the first meters of sliding, several other investigations identified in low pressure air environment the highest CoF values as well [16, 24, 45]. Moreover, the combination of abrasive wear and corrosion is

evidently affecting the tribology even when using corrosion resistant steel, as the passivation layer (oxide film of 1 to 3 nm thickness) is continuously damaged and reshaped [46]. At room temperature and without an electrolyte, the so-called low temperature corrosion is typically decreasing with increasing oxide layer thickness and thus limited to the mentioned upper surface layer. Nevertheless, during the experiments, the wear debris as well as the contact surfaces were crushed and furrowed several times, forming continuously new areas susceptible for corrosion. In addition, caused by the friction, approx. 0.01 W heat is generated per wear contact, which results in relation to the contact area in a total heating power of approx. 3.5 $kW \cdot m^{-2}$. Taking the real contact surface at the asperites (microcontacts) into account, the arising peak temperatures can therefore influence the wear significantly [47]. Furthermore, the corrosion itself as an exothermic reaction contributes to local high temperatures. These reactions could be retraced in the EDX and XPS measurements as well, showing an increase of iron oxides. Especially the wear debris contained more oxygen than iron at low chromium and carbon content (see Fig. 10 and Table 2), indicating the formation of Fe_2O_3 (see brownish color in Figs. 6 and 8). At high air pressure, the friction increased faster compared to the experiments at ambient pressure and the wear rate was significantly higher. This can be explained by faster ongoing corrosion processes, as at high pressure more oxygen is present at the loaded surfaces and in the contact areas. Regarding the wear at the balls, high wear rates also raised the question of the consistency of the specimen hardness with ongoing wear. Nanoindentation measurements at flattened balls showed no decrease of material hardness even at the highest occurring wear within this investigation.

4.2 Tribological effects in liquid and gaseous CO_2

In CO_2 environment at ambient pressure, two different friction levels can be observed: First, a typical friction–time behavior (see Fig. 5 and Ref. [48]) as the CoF increases significantly and reaches an almost constant level after approx. 300 seconds. At the beginning of the experiment, existing oxidic surface layers and contaminants mainly define the CoF. If this layer is rutted, adhesion effects occur, leading to increasing friction. In second prospective, the CoF stays almost constant at low level during the experiment. In this case, a separation of the counter bodies by a surface layer can be assumed during the whole time of the experiments, meaning that no significant adhesion effects occur. In Ausserer et al. [49], a similar friction behavior in CO_2 atmosphere at ambient pressure is presented. The CO_2 molecule is relatively inert and has no electric dipole moment, so it weakly adsorbs on clean iron surfaces [50, 51]. Nevertheless, the Van der Waals interaction is comparably high [52] and in combination with oxygen, e.g. on iron or chromium oxide surface layers, CO_2 adsorbs well (see Refs. [53, 54], and exemplarily for adsorption models Refs. [25, 55]). Since the surface of the specimens is naturally covered with a thin metal oxide layer [56] and as described in Mishina [14] and Huo et al. [57] (in combination with carbon films), this may lead to a thin recovering CO_2 surface layer. If the load of the contact is too high, this layer is potentially directly ruptured. At high contact frequencies, the layer cannot recover completely before the next erosion and is thus removed over time. The investigations showed that an increase of atmospheric pressure seems to support the recovering of this CO_2 surface layer. The recovering effect was confirmed in measurements over a sliding distance of more than 100 m, which resulted in no significant increase of the CoF and wear. In Fig. 13, an SEM image of a worn specimen, tested in air and one in GCO_2 atmosphere (at p_F = 6 MPa and after a sliding distance of 90 m) is shown, respectively. This demonstrates very distinctly the reduction of wear when using CO_2 compared to air atmosphere. However, the wear in CO_2 increased with rising fluid pressure as well. Similar to the effects in air environment, intensified chemical corrosion at the loaded areas occurred (see Fig. 7), since more CO_2 is present at the surfaces. Existing iron oxide may react with the CO_2 to iron(II) carbonate [25]. This can also be stated by the whitish color of the wear debris around the flattening of the balls (see Fig. 6). Furthermore, the EDX measurement of the specimen worn in CO_2 (Fig. 10), showed high carbon contents, especially at the wear debris. Although, the high hydrocarbon content in the XPS measurements

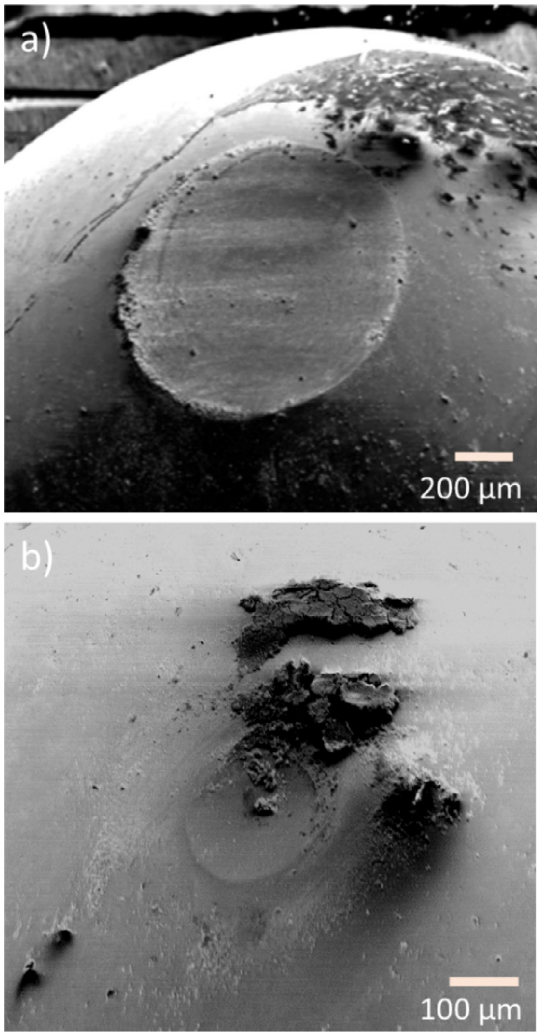

Fig. 13 Images (SEM) of the flattened balls and wear debris after a sliding distance of 90 m in 6 MPa (a) pressurized air atmosphere and (b) GCO_2 atmosphere (note the different magnifications).

(result of low wear, see Table 2) impede the exact C allocation, an increase of iron carbonates on the surface is obvious when using CO_2. This can be seen in higher carbon and oxygen combined with lower iron contents in accordance with the shift in the binding energies [42]. Investigations regarding ongoing Fischer-Tropsch processes at the metal surfaces in high pressure CO_2 atmosphere (see Ref. [58]) could explain high hydrocarbon contents, but no evident hydrogen source was identified to support this hypothesis. Since the iron carbonate forms primarily from limited iron oxide, the corrosion decreases over time and is, in comparison with the behavior in air environment, significantly lower. Furthermore, the formed iron carbonates have a lower material hardness compared to the iron oxides and can thus act like a solid lubricant [59]. The adsorbed surface layers in combination with the formation of carbonates trigger mild wear and can explain the decrease in surface roughness of the disc in CO_2 environment, like a polishing effect (see Fig. 9). Comparable effects and only low adhesive wear were also investigated by Zhang and Jourani [16] who examined the tribological behavior of dual-phase steel in 0.1 MPa CO_2 atmosphere. The experiments in LCO_2 showed a tendency to slightly higher CoF and lower wear compared to the gaseous state at 6 MPa fluid pressure. An explanation can be the increased viscosity and shear stress of the fluid. In addition, as discussed before, the arising peak temperatures at the contact surfaces have a direct impact on adhesion phenomena. Since CO_2 has a comparatively high heat capacity at 6 MPa, the temperatures could be significantly lower in comparison to other fluids and therefore result in a different tribological behavior. When using LCO_2, rising temperatures inside the interstice may lead to evaporation processes. Though, so far, no significant differences in tribology could be determined regarding the state of CO_2 at 6 MPa fluid pressure in this investigation. Nunez et al. [25] and Demas and Polycarpou [28] also investigated the lubricity of CO_2 at high pressure levels for the use as a refrigerant and determined lower friction and wear at elevated pressure and temperature levels (even in the area of the gas–liquid transition line in the p–T phase diagram). In contrast, to reduce friction and wear, Wu et al. [59] identified an optimum CO_2 pressure regarding friction and wear at 0.02 MPa to 0.05 MPa, arguing with an increased wear at higher pressures. Even though the results of this investigation showed also slightly higher chemical wear with increasing pressure, significantly lower CoF were measured. Thus, higher CO_2 fluid pressures seem to be advantageous for lubricating processes like dry deep drawing.

4.3 Tribological effects in nitrogen environment

The tribological behavior in N_2 showed completely different characteristics than that in air environment. This can be attributed to the absence of oxygen. In Mishina [14, 15] and other studies [60, 61], a comparable

behavior is shown in low atmospheric pressure (vacuum). The tribological behavior is driven by adhesive effects, as the wear debris stay in the friction zone and no adsorbed surface layer forms. Thus, usually the CoF is at high and the wear rate at low level at this point. With increasing environmental pressure, the CoF decreases counteractively to increasing wear, as atmospheric molecules adsorb on the surfaces and benefit the removal of the debris from the contact zone. At some point with rising pressure and dependent of the adsorption effects, the growing surface layer is sufficient to decrease wear again. In comparison to the previously discussed fluids (air/oxygen and CO_2), N_2 has a weak adsorption activity on metals [15]. Thus, it was assumed that a high environmental pressure is needed [62] to reduce friction and wear effectively. Having said this, our measurements showed even at the high pressure level of 6 MPa, no reduction of the CoF or the wear compared to ambient pressure. Therefore, N_2 seems to form no tribological effective adsorbed surface layer before condensation occurs. Transferred to effects in deep drawing [10] and LN_2 cryogenic machining [63] this means a lubrication only driven by temperature drop and flow properties of the medium. For chemical reactions of iron and N_2, usually temperatures above 800 K are required. Thus, as expected, the EDX and XPS measurements (see Fig. 10 and Table 2) showed comparable results to the reference or to the experiments in Ar environment, indicating that no significant chemical changes of the material occurred during wearing in N_2 environment. The increased amount of chromium is caused by transfer e.g. adhesive effects from the disc to the ball, since the chromium content of the disc steel (X155CrVMo12-1) is considerably higher. Thus, the chemical analysis in combination with the shown unstable wear effects (see Fig. 7) and comparably large debris size (see Ref. [21]) lead to the assumption of a high influence of adhesion wear in N_2 environment. In addition, no clear indications of an adsorbed surface layer could be found. At 0.1 MPa environmental pressure, the measured CoF and wear tended to be lower than that in high pressure atmosphere. This may be explained by a higher influence of the approx. 300 nm thick oxide surface layer and contaminations (mainly aliphatic carbon and water) of the specimens at the beginning of the experiments [56]. Overall, a high similarity of the tribological behavior in N_2 and Ar environment was determined, comparable to the results of Zhang and Jourani [16] at low fluid pressure. It can be suggested that N_2 environment pressures considerably higher than 6 MPa are needed to effectively reduce friction and wear at room temperature.

4.4 Tribology in argon atmosphere

As previously mentioned, in Ar environments, comparable effects like in N_2 atmosphere occurred. The inert gas prevents chemical reactions between the specimen surfaces and the environment during the tribological experiment. Furthermore, at room temperature no adsorption layer is probable. Thus, the chemical changes (see Fig. 10) of the surfaces are exclusively caused by mechanical wear effects. The increase of chromium and nitrogen is again a result of adhesive wear and material transfers from the disc to the ball (see Chapter 4.3 and Table 2). These effects also cause the slight decrease of the carbon content since previous surface contaminants were removed. As long as the surface top layer of oxides and contaminants is intact, low friction and wear values were measured. However, as soon as this layer was disrupted, strong adhesion occurred leading to high friction values (see Fig. 12 arith. mean of last 100 s) and deep furrows in the specimen discs (see Fig. 8), comparable to tribology in vacuum [15, 33, 61]. This is characterized by high CoF and moderate wear because of dominating adhesive tribological effects, which can be seen also in the big error bars of the wear rates in Fig. 7. The CoF as well as the wear rate measurements lead to the assumption of increasing values with increasing fluid pressure, comparable to the effects in N_2 environment. Since no significant adsorption effects of Ar on the surfaces are probable at room temperature, consistent severe friction and wear was expected [15]. It is supposed that this increase is caused by viscosity increase of the fluid and by the decreasing effect of the previous surface layer (dilution effects). Nevertheless, as discussed, the adhesion effects lead to a high inconsistency of the experiments and thus allow no clear conclusion about the influence of the fluid pressure on tribological behavior in Ar environment.

5 Conclusions

The influence of different fluid environments at ambient and high pressure level on tribological behavior of dry sliding steel contacts was investigated using a novel high-pressure tribometer. Regarding the impact of the fluid on the tribological behavior in ambient pressure, fundamental differences were revealed:

In air environment, the oxygen content triggers tribo-corrosion effects at the loaded surfaces, as shown in increasing amounts of iron oxides. The hardness of the particles is comparable to the disc material, leading in turn to enhanced abrasive wear. Within this study, no lubrication effects of the debris could be determined.

In CO_2 environment, adsorption processes are suggested, leading to a self-recovering surface layer, reducing the direct contact of the solids and thus result in low CoF and wear values. At ambient pressure, the recovering is usually not sufficient to create a long-term stable tribolayer. If the surface oxide layer is reduced due to wear, the recovery decreases. Thus, the CoF frequently increases continuously over the time. Furthermore, the formation of carbonates acting as a solid lubricant at the loaded surfaces could be observed. However, tribo-corrosion showed no significant influence and the wear stayed on a low level, resulting in the lowest measured wear of all experiments.

In N_2 and Ar environments, almost similar tribological behavior was observed. The gases trigger no chemical reactions on the surfaces and even with N_2 no significant effect of an adsorbed surface layer was measurable. As soon as the original surface oxide layer was rutted, strong adhesion between the solids occurred, leading to tribological effects comparable to those of clean metal surfaces in vacuum.

Dependent on the described tribological behavior at ambient pressure, these were enhanced by an increase of the fluid pressure up to 6 MPa. Since in air environment more oxygen is present inside the friction zone at higher pressure level, intensified corrosion effects were measured leading to significantly higher CoF and wear. In contrast, in CO_2 environment increasing fluid pressure led to a reduction of the CoF since the recovering of the adsorbed surface layer appears to be enhanced and an increased formation of carbonates was measurable. In turn, this reaction also led to intensified chemical wear. At 6 MPa, the lowest CoF was measured in GCO_2 atmosphere, the lowest wear in LCO_2, though no significant differences regarding the state of CO_2 could be measured within this investigation. In case of N_2 and Ar, increasing pressure showed no significant influence on the tribological behavior. Thus, it is suggested that especially for N_2 higher fluid pressures are required to reduce friction and wear measurably.

Regarding the ability of the different media to lubricate dry deep drawing processes, air seems highly unfavorable because of high CoF and wear rates. As long as the surface oxide layer stays intact, CoF and wear in N_2 and Ar environment is tolerable for deep drawing processes. Nevertheless, at high contact pressures, this layer gets disrupted and the tribology is characterized by adhesion effects. Thus, for slightly loaded processes, these gases can be an opportunity, but for high loaded contacts, they seem disadvantageous. The most promising results were achieved using CO_2. Especially, at high fluid pressure like during deep drawing processes, the use of CO_2 is beneficial. Thus, CO_2 lubrication can contribute to low friction values, resulting in high drawing depths and an extended tool life.

Funding

The scientific investigations of this paper were funded by the German Research Foundation (DFG) within the priority program SPP 1676 Dry Metal Forming-Sustainable Production by Dry Processing in Metal Forming. We thank the DFG for the funding of this research project. Furthermore, the authors would like to thank the DFG for the provision of the pressure vessel, which was used to assemble the high-pressure tribometer and therefore being an essential component to this work.

Acknowledgements

For the possibility and the helpful assistance regarding the 3D topographic surface measurements we thank the Institute for Metal Forming Technology (IFU,

University of Stuttgart); especially Gerd Reichardt. In addition, we would like to thank the IGB and IGVP colleagues Mateus Oliveira Moneta and Felix Remppel for the discussions to the tribometer design as well as Linus Stegbauer and Alexander Southan for helpful exchanges and support regarding procurement and analytics. Furthermore, we thank Jan Hinnerk Henze for his support and the profound discussions. His assistance was especially helpful concerning the chemical analysis.

Declaration of competing interest

The authors have no competing interests to declare that are relevant to the content of this article.

References

[1] Nagendramma P, Kaul S. Development of ecofriendly/ biodegradable lubricants: An overview. *Renew Sustain Energy Rev* **16**(1): 764–774 (2012)

[2] Rani S, Joy M L, Nair K P. Evaluation of physiochemical and tribological properties of rice bran oil–biodegradable and potential base stoke for industrial lubricants. *Ind Crops Prod* **65**: 328–333 (2015)

[3] Botas J A, Moreno J, Espada J J, Serrano D P, Dufour J. Recycling of used lubricating oil: Evaluation of environmental and energy performance by LCA. *Resour Conserv Recycl* **125**: 315–323 (2017)

[4] Bay N, Azushima A, Groche P, Ishibashi I, Merklein M, Morishita M, Nakamura T, Schmid S, Yoshida M. Environmentally benign tribo-systems for metal forming. *CIRP Ann* **59**(2): 760–780 (2010)

[5] Freiße H, Ditsche A, Seefeld T. Reducing adhesive wear in dry deep drawing of high-alloy steels by using MMC tool. *Manufacturing Rev* **6**: 12 (2019)

[6] Prünte S, Music D, Terziyska V L, Mitterer C, Schneider J M. Molecular coverage determines sliding wear behavior of *n*-octadecylphosphonic acid functionalized Cu–O coated steel disks against aluminum. *Materials* (*Basel*) **13**(2): 280 (2020)

[7] Vollertsen F, Schmidt F. Dry metal forming: Definition, chances and challenges. *Int J Precis Eng Manuf Green Technol* **1**(1): 59–62 (2014)

[8] Zahedi E, Woerz C, Reichardt G, Umlauf G, Liewald M, Barz J, Weber R, Foerster D J, Graf T. Lubricant-free deep drawing using CO_2 and N_2 as volatile media injected through laser-drilled microholes. *Manufacturing Rev* **6**: 11 (2019)

[9] Reichardt G, Henn M, Reichle P, Hemming D, Umlauf G, Riedmüller K, Weber R, Barz J, Liewald M, Graf T, et al. Investigations on the process stability of dry deep drawing with volatile lubricants injected through laser-drilled microholes. In Proceedings of the TMS 150th Annual Meeting & Exhibition Supplemental Proceedings, 2021: 230–246.

[10] Reichle P, Reichardt G, Henn M, Umlauf G, Barz J, Riedmüller K R, Liewald M, Tovar G E M. Volatile lubricants injected through laser drilled micro holes enable efficiently hydrocarbon-free lubrication for deep drawing processes. *Int J Precis Eng Manuf Green Technol* **10**(4): 875–890 (2023)

[11] Reichardt G, Henn M, Reichle P, Umlauf G, Riedmüller K, Weber R, Barz J, Liewald M, Graf T, Tovar G E M. Friction and wear behavior of deep drawing tools using volatile lubricants injected through laser-drilled micro-holes. *JOM* **74**(3): 826–836 (2022)

[12] Frank Philip Bowden F P, Hughes T P. The friction of clean metals and the influence of adsorbed gases. The temperature coefficient of friction. *Proc R Soc Lond A* **172**(949): 263–279 (1939)

[13] Iwabuchi A, Kayaba T, Kato K. Effect of atmospheric pressure on friction and wear of 0.45% C steel in fretting. *Wear* **91**(3): 289–305 (1983)

[14] Mishina H. Chemisorption of diatomic gas molecules and atmospheric characteristics in adhesive wear and friction of metals. *Wear* **180**(1–2): 0043164895800034 (1995)

[15] Mishina H. Atmospheric characteristics in friction and wear of metals. *Wear* **152**(1): 99–110 (1992)

[16] Zhang Y, Jourani A. Combined effect of microstructure and gaseous environments on oxidative and adhesive wear of dual-phase steel. *J Mater Eng Perform* **30**(12): 9333–9351 (2021)

[17] Mello, J.D.B. de, Binder, R. Tribolayer Formed on Multifunctional Coatings: Influence of the Environment. *Tecnologia em Metalurgia Materiais e Mineração* **9**(2): 81–88, https://doi.org/10.4322/tmm.2012.013 (2012) (in Portuguese)

[18] Zhou S G, Wang L P, Xue Q J. Testing atmosphere effect on friction and wear behaviors of duplex TiC/a-C(Al) nanocomposite carbon-based coating. *Tribol Lett* **47**(3): 435–446 (2012)

[19] Hübner W, Gradt T, Schneider T, Börner H. Tribological behaviour of materials at cryogenic temperatures. *Wear* **216**(2): 150–159 (1998)

[20] Pereira O, Rodríguez A, Fernández-Abia A I, Barreiro J, López de Lacalle L N. Cryogenic and minimum quantity lubrication for an eco-efficiency turning of AISI 304. *J Clean Prod* **139**: 440–449 (2016)

[21] Velkavrh I, Ausserer F, Klien S, Brenner J, Forêt P, Diem A. The effect of gaseous atmospheres on friction and wear of steel–steel contacts. *Tribol Int* **79**: 99–110 (2014)

[22] Kazachkin D V, Nishimura Y, Irle S, Feng X, Vidic R, Borguet E. Temperature and pressure dependence of molecular adsorption on single wall carbon nanotubes and the existence of an "adsorption/desorption pressure gap". *Carbon* **48**(7): 1867–1875 (2010)

[23] Mistry H, Behafarid F, Bare S R, Roldan Cuenya B. Pressure-dependent effect of hydrogen adsorption on structural and electronic properties of Pt/γ-Al_2O_3 nanoparticles. *ChemCatChem* **6**(1): 348–352 (2014)

[24] De Mello J D B, Binder R, Demas N G, Polycarpou A A. Effect of the actual environment present in hermetic compressors on the tribological behaviour of a Si-rich multifunctional DLC coating. *Wear* **267**(5–8): 907–915 (2009)

[25] Nunez E E, Polychronopoulou K, Polycarpou A A. Lubricity effect of carbon dioxide used as an environmentally friendly refrigerant in air-conditioning and refrigeration compressors. *Wear* **270**(1–2): 46–56 (2010)

[26] Lee K M, Suh A Y, Demas N G, Polycarpou A A. Surface and sub-micron sub-surface evolution of Al390-T6 undergoing tribological testing under submerged lubrication conditions in the presence of CO_2 refrigerant. *Tribol Lett* **18**(1): 1–12 (2005)

[27] Demas N G, Polycarpou A A. Ultra high pressure tribometer for testing CO_2Refrigerant at chamber pressures up to 2000 psi to simulate compressor conditions. *Tribol Trans* **49**(3): 291–296 (2006)

[28] Demas N G, Polycarpou A A. Tribological investigation of cast iron air-conditioning compressor surfaces in CO_2 refrigerant. *Tribol Lett* **22**(3): 271–278 (2006)

[29] ChemicaLogic Corporation. Carbon Dioxide Phase Diagram, from http://www.chemicalogic.com/Pages/DownloadPhaseDiagrams.html, May 16, 2023.

[30] Sugimura J, Ono B, Hashimoto M, Tanaka H, Yamamoto Y. (2005) Sliding experiments of steels in gaseous hydrogen. *Life Cycle Tribology*. Amsterdam: Elsevier: 465–473

[31] German standard DIN 51834-2:2017-05. Testing of lubricants—Tribological test in the translatory oscillation apparatus—Part 2: Determination of friction and wear data for lubricating oils. Beuth Verlag GmbH, Berlin, 2014: https://doi.org/10.31030/2643102. (In German)

[32] Khun N W, Tan A W Y, Liu E. Mechanical and tribological properties of cold-sprayed Ti coatings on Ti-6Al-4V substrates. *J Therm Spray Technol* **25**(4): 715–724 (2016)

[33] Velkavrh I, Ausserer F, Klien S, Voyer J, Ristow A, Brenner J, Forêt P, Diem A. The influence of temperature on friction and wear of unlubricated steel/steel contacts in different gaseous atmospheres. *Tribol Int* **98**: 155–171 (2016)

[34] Hameed Sultan M T, Mohd Jamir M R, Abdul Majid M S, Azmi A I, Saba N. *Tribological Applications of Composite Materials*. Springer Singapore, 2021. https://doi.org/10.1007/978-981-15-9635-3.

[35] German standard DIN 5401:2002-08. Rolling bearings—Balls for rolling bearings and general industrial use. Beuth Verlag GmbH, Berlin, 2002: https://doi.org/10.31030/9272444. (In German)

[36] Reichardt G, Wörz C, Singer M, Liewald M, Henn M, Förster D J, Zahedi E, Boley S, Feuer A, Onuseit V, et al. Tribological system for cold sheet metal forming based on volatile lubricants and laser structured surfaces. *Dry Metal Forming Open Access Journal* **6**: 128–165, https://doi.org/10.26092/elib/156 (2020)

[37] Ramqvist L, Hamrin K, Johansson G, Fahlman A, Nordling C. Charge transfer in transition metal carbides and related compounds studied by ESCA. *J Phys Chem Solids* **30**(7): 1835–1847 (1969)

[38] Wagner C D, Gale L H, Raymond R H. Two-dimensional chemical state plots: A standardized data set for use in identifying chemical states by X-ray photoelectron spectroscopy. *Anal Chem* **51**(4): 466–482 (1979)

[39] Solomon J L, Madix R J, Stöhr J. Orientation and absolute coverage of furan and 2, 5-dihydrofuran on Ag(110)

determined by near edge X-ray absorption fine structure and X-ray photoelectron spectroscopy. *J Chem Phys* **94**(5): 4012–4023 (1991)

[40] Guo S Q, Xu L N, Zhang L, Chang W, Lu M X. Corrosion of alloy steels containing 2% chromium in CO_2 environments. *Corros Sci* **63**: 246–258 (2012)

[41] Paparazzo E. XPS and auger spectroscopy studies on mixtures of the oxides SiO_2, Al_2O_3, Fe_2O_3 and Cr_2O_3. *J Electron Spectrosc Relat Phenom* **43**(2): 97–112 (1987)

[42] Heuer J K, Stubbins J F. An XPS characterization of $FeCO_3$ films from CO_2 corrosion. *Corros Sci* **41**(7): 1231–1243 (1999)

[43] Medical statistics: A guide to data analysis and critical appraisal. *Ann R Coll Surg Engl* **88**(6): 603 (2006)

[44] Cai Z B, Zhu M H, Zheng J F, Jin X S, Zhou Z R. Torsional fretting behaviors of LZ50 steel in air and nitrogen. *Tribol Int* **42**(11–12): 1676–1683 (2009)

[45] Shi J, Gong Z B, Wang C B, Zhang B, Zhang J Y. Tribological properties of hydrogenated amorphous carbon films in different atmospheres. *Diam Relat Mater* **77**: 84–91 (2017)

[46] Landolt D. *Corrosion and Surface Chemistry of Metals*. Lausanne, (Switzerland): EPFL Press, 2007.

[47] Popov V L. *Contact Mechanics and Friction: Physical Principles and Applications*. Springer, 2017. https://doi.org/10.1007/978-3-662-53081-8_13.

[48] Czichos H, Habig K H. *Tribologie-Handbuch: Tribometrie, Tribomaterialien, Tribotechnik*. Wiesbaden (Germany): Springer Fachmedien Wiesbaden, 2020. (In German).

[49] Ausserer F, Klien S, Velkavrh I, Forêt P, Diem A. Investigations of the sliding and wear behaviour in various gaseous atmospheres using a SRV testing apparatus. *Tribologie und Schmierungstechnik* **63**(1): 22–28 (2016)

[50] Solymosi F. The bonding, structure and reactions of CO_2 adsorbed on clean and promoted metal surfaces. *J Mol Catal* **65**(3): 337–358 (1991)

[51] Zhang C, Sunarso J, Liu S M. Designing CO_2-resistant oxygen-selective mixed ionic–electronic conducting membranes: Guidelines, recent advances, and forward directions. *Chem Soc Rev* **46**(10): 2941–3005 (2017)

[52] Banerjee S, Sutanto S, Kleijn J M, van Roosmalen M J E, Witkamp G J, Stuart M A. Colloidal interactions in liquid CO_2: A dry-cleaning perspective. *Adv Colloid Interface Sci* **175**: 11–24 (2012)

[53] Bonenfant D, Kharoune L, Sauvé S, Hausler R, Niquette P, Mimeault M, Kharoune M. Molecular analysis of carbon dioxide adsorption processes on steel slag oxides. *Int J Greenh Gas Contr* **3**(1): 20–28 (2009)

[54] Petrovic B, Gorbounov M, Masoudi Soltani S. Influence of surface modification on selective CO_2 adsorption: A technical review on mechanisms and methods. *Microporous Mesoporous Mater* **312**: 110751 (2021)

[55] Burghaus U. Surface chemistry of CO_2–Adsorption of carbon dioxide on clean surfaces at ultrahigh vacuum. *Prog Surf Sci* **89**(2): 161–217 (2014)

[56] Abdelbary A. *Extreme Tribology: Fundamentals and Challenges*. CRC Press Taylor & Francis Group, 2020.

[57] Huo L, Wang S H, Pu J B, Sun J H, Lu Z B, Ju P F, Wang L P. Exploring the low friction of diamond-like carbon films in carbon dioxide atmosphere by experiments and first-principles calculations. *Appl Surf Sci* **436**: 893–899 (2018)

[58] Dorner R W, Hardy D R, Williams F W, Davis B H, Willauer H D. Influence of gas feed composition and pressure on the catalytic conversion of CO_2 to hydrocarbons using a traditional cobalt-based fischer–tropsch catalyst. *Energy Fuels* **23**(8): 4190–4195 (2009)

[59] Wu X, Cong P, Nanao H, Minami I, Mori S. Tribological behaviors of 52100 steel in carbon dioxide atmosphere. *Tribol Lett* **17**(4): 925–930 (2004)

[60] Buckley D H. *Friction, Wear, and Lubrication in Vacuum*, Cleveland (USA): NASA Special Publication 277, 1971.

[61] Miyoshi K. Considerations in vacuum tribology (adhesion, friction, wear, and solid lubrication in vacuum). *Tribol Int* **32**(11): 605–616 (1999)

[62] Menon P G. Adsorption at high pressures. *Chem Rev* **68**(3): 277–294 (1968)

[63] Jun S C. Lubrication effect of liquid nitrogen in cryogenic machining friction on the tool-chip interface. *J Mech Sci Technol* **19**(4): 936–946 (2005)

Paul REICHLE. He is a research engineer at Fraunhofer Institute for Interfacial Engineering and Biotechnology (IGB) in the Department of Functional Surfaces and Materials as well as a doctoral candidate at the Institute of Interfacial Process Engineering and Plasma Technology (IGVP) at the University of Stuttgart, Germany. He studied sustainable engineering and mechanical engineering at the Universities of Applied Sciences Esslingen and Konstanz (both Germany), respectively. His research focus is on surface modification and plasma coatings for reducing friction, wear and to adjust wetting properties.

Jakob BARZ. He is Senior Scientist at the Fraunhofer Institute for Interfacial Engineering and Biotechnology (IGB), Germany, and principal investigator at the Institute for Interfacial Process Engineering and Plasma Technology (IGVP) at University of Stuttgart, Germany. He joined Fraunhofer in 2003 after finishing his Diploma in physics at University of Stuttgart. In 2010, he received his Ph.D. degree on a plasma-chemical topic at the former Institute for Plasma Research (IPF), Germany. His focusses of research are plasma processes as well as surface and interface analysis.

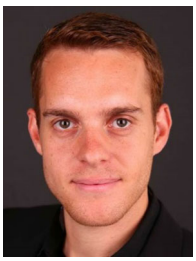

Georg UMLAUF. He has been at Fraunhofer IGB since 2013. Umlauf studied mechatronics, specializing in "special manufacturing methods", at the Dresden University of Technology (TUD), Germany. In 2020, he completed his Ph.D. degree in process engineering with studies on the application of carbon dioxide as a volatile lubricant in dry metal forming at the Institute of Interfacial Process Engineering and Plasma Technology (IGVP) at the University of Stuttgart, Germany. Since 2018, he has been working as a researcher in the innovation field of functional surfaces and materials in the Department of Plasma Processes at the Fraunhofer Institute IGB in Stuttgart.

Günter E.M. TOVAR. He directs the Institute of Interfacial Process Engineering and Plasma Technology (IGVP) at the University of Stuttgart, Germany, since 2015. Previously, he studied chemistry with a focus on physical chemistry and chemical technology at the Technical University of Darmstadt, Germany, the Université de Bordeaux and at the CNRS CEMES in Toulouse, both France. He conducted his doctorate at the Max Planck Institute for Polymer Research and the Johannes-Gutenberg-University in Mainz, Germany, and at RIKEN, the Institute of Physical and Chemical Research, Wako near Tokyo, Japan, and habilitated at the University of Stuttgart. His research interests include nanomaterials technology, medical technology, and environmental engineering, and he draws inspiration from the United Nations Sustainable Development Goals.